

Gold Nanoparticles Decorated With Octreotide For Somatostatin Receptors Targeting

Ahmed A. H. Abdellatif, Saleh Abd El Rasoul and Shaaban Osman

*Faculty of Pharmacy, Department of Pharmaceutics and Industrial pharmacy,
Al-Azhar University, Assuit, Egypt.*

Abstract

Targeted drug delivery systems increase the accumulation of medication in the targeted tissues. In contrast, they reduce the relative concentration of medication in non-targeted tissues and inhibit the non-specific distribution to both liver and spleen. The aim of this study is to formulate nanoparticles that are selectively capable of reaching specific sites in the human body via receptors for either diagnostic or therapeutic purposes. These nanoparticles were loaded with octreotide (OCT) which are carried to somatostatin receptor cells. The formulated nanoparticles were characterized by dynamic light scattering (DLS) and UV-VIS spectroscopy. The cellular uptake of the formulated gold nanoparticles (AuNPs-OCT) were studied on cell line with well-expressed somatostatin receptors using inductively coupled plasma optical emission spectroscopy (ICP-OES). The results of DLS showed a successful coating of OCT on the AuNPs, since the average diameter of the AuNPs was increased uniformly. Additionally, the inversion of the zeta potential sign is a further indicator for successful attachment of OCT. The UV-VIS absorption spectra showed a red shift in the surface plasmon resonance peak of AuNPs-OCT compared to unmodified AuNPs. Furthermore, ICP-OES results showed that the counted number of AuNPs-OCT particles per cell is significantly higher than that in case AuNPs-citrate and AuNPs-OCT in the presence of antagonists. Interestingly, it has been observed that the number of particles decreased hugely to the extent which is similar to unmodified AuNPs upon addition of antagonist. The obtained results indicated that the binding of modified nanoparticles to cells is due to differences in surface properties and not to differences in size.

1. INTRODUCTION

Nanoparticles are the particles of such material having dimensions of about 100 nm or less, they do not only have a characteristic size but also a unique surface chemistry(1). Nanoparticles have major advantages in targeted drug delivery compared to other systems. So a lot of effort to formulate nanoparticles which are capable of selectively reaching specific sites in the human body via receptor targeting for diagnostic as well as therapeutic purposes were done. Especially gold nanoparticles (AuNPs) were chosen as a model of nanoparticles due to their inherent properties making them a good nano carriers for drug delivery(2).

AuNPs are very important and applicable tool in nanotechnology, due to their easy surface functionalization or easy bio-conjugation, their stability and biocompatibility. Recently, decorations of AuNPs expand their application as potential biomedical applications, including biosensors, bioimaging, photothermal therapy, and targeted drug delivery(3). Especially decoration of AuNPs with octreotide (OCT) which is a synthetic somatostatin (SST) analogue acting as a selectively agonist targeted and delivered AuNPs to the specific sites with high efficacy.

It selectively binds to SSTR2, SSTR5. In this study, OCT was selected and not the natural SST, due to the plasma half-life of OCT is much higher than that of the endogenous SST (4). Due to easy conjugation of OCT than SST, many studies reported that OCT was delivered to cancer cells that express SSTRs (5). In previous study, [Tyr]³Octreotide (TOC) was conjugated to micellar nanoparticles for the targeting of specific malignant tumor cells (6-7).

SSTRs are members of the G protein coupled receptors (GPCRs) super family. There are five different subtypes of SSTRs (SSTR1-5), SSTR2 having been classified into two subtypes, SSTR_{2A} and SSTR_{2B} (8-9). The five receptor subtypes bind with the natural SST and its analogues with low nanomolar affinity, and produce defined biological effects in many normal and diseased cells (10). The blocking of SSTRs with antagonist suppresses the interaction of the peptide agonist with SSTRs (11).

Ultraviolet-visible spectroscopy (UV-VIS spectroscopy) is a very important technique that allows for the estimation of the size of AuNPs, concentration, and aggregation level, because the surface plasmon resonance (SPR) effects depends on the shape, size, and aggregation of AuNPs (12-15). They have been the subject of many studies and many applications in medicine and in biology, such as immunoassays, biomedical chemistry, photothermalysis, drug targeting of cancer cells and in biomedical research (16-17).

Tumor cells can be killed by excitation of internalized AuNPs (18). Ligands-decorated AuNPs can also target special receptors in the human body, i.e. transferrin receptor present in the microvascular endothelial cells of the blood-brain barrier (19). AuNPs were delivered to ovarian cancer cells that express the epidermal growth factor receptor and the folate receptor (20). Conjugation of AuNPs to receptor specific peptides could be useful and helpful in the therapy of tumor cells expressing somatostatin receptors (SSTRs). AuNPs can be used to optimize the biodistribution of drugs to diseased organs, tissues or cells, in order to improve and target drug delivery. In our work, the aim was to formulate OCT decorated AuNPs as targeted drug delivery system. OCT substituted

at the amine group of its N-terminus by 11-Mercaptoundecanoic acid (11-MUA) producing mono-substituted OCT-MUA. OCT-MUA was deposited on the gold surface to form OCT-AuNPs. Characterization of the formulated AuNPs-OCT was studied using dynamic light scattering and UV-VIS spectroscopy. Also in the present study cellular uptake of the formulated AuNPs-OCT was studied on cell line with well-expressed somatostatin receptors using inductively coupled plasma optical emission spectroscopy (ICP-OES).

Moreover this work focused on the methods of preparation, the characterization of the formulated nanoparticles, cellular uptake experiments.

2. MATERIAL AND METHODS

2.1 Materials

Octreotide acetate (OCT) was purchased from ChemPep (Wellington, USA). Hydrogen tetrachloroaurate tri-hydrate ($\text{HAuCl}_4 \cdot 3\text{H}_2\text{O}$), 11-Mercaptoundecanoic acid (11-MUA), Dulbecco's phosphate buffered saline (pH 7.4), Diisopropylethylamine (DIPEA), bovine serum albumen and cyn-154806 trifluoroacetate were purchased from Sigma Aldrich (Steinheim, Germany). Trisodium citrate dihydrate, sodium chloride, nitric acid, hydrochloric acid, sodium dihydrogen phosphate, disodium hydrogen phosphate were purchased from Merck (Darmstadt, Germany). The ultrafiltration units of a 100-kDa MWCO membrane were purchased from Amicon Ultra-4 Millipore (Billerica, MA). Dialysis spectra/pro CE float analyzer (MWCO: 100-500 Da) was purchased from Rancho Dominguez (California, USA). Pancreatic carcinoid tumor cells (BON-1) were kindly supplied by Haematology department (Regensburg, Germany). All glassware was thoroughly washed with freshly prepared aqua regia ($\text{HCl}:\text{HNO}_3$, 3:1), rinsed with Millipore water several times and then dried at 50 °C for 2-3 hours.

2.2 Preparation and characterization of AuNPs loaded with OCT

2.2.1 Preparation of AuNPs-citrate

AuNPs were prepared by reduction of $\text{HAuCl}_4 \cdot 3\text{H}_2\text{O}$ by trisodium citrate, according to the previously reported procedure (21-22). Briefly, 3ml of 38.8 mM trisodium citrate solution were added to 100 ml of 0.3 mM $\text{HAuCl}_4 \cdot 3\text{H}_2\text{O}$ solution in 250 ml round flask. The reaction mixture stirred vigorously and heated under reflux. After 15 minutes, the prepared AuNPs was left to cool at room temperature with continuous stirring for further 15 minutes. AuNPs were purified from larger aggregates by centrifugation for 30 minutes at $2,450 \times g$ using (Avanti centrifuge J-E/ Beckman coulter GmbH, Germany) (23).

2.2.2 N-terminal mono-substitution of OCT with 11-MUA

OCT is usually PEGylated at its N-terminus but not at the Lys side chain due to the later is essential for OCT activity. Specific PEGylation of OCT at the N-terminus is based on the difference in reactivity between the amino group in the N-terminus (pKa 7.8) and the other one in Lys residue (pKa 10.1) at acidic pH (24-27). To be easy deposited on the

gold surface, OCT was mono-substituted with 11-MUA at N-terminal according to the previously reported method (28). In brief, 3 ml (1 μM) OCT was mixed with 3 ml (1 μM) purified 11-MUA in 25 ml rounded-bottom flask. To the reaction mixture, NHS and EDC in 2-fold excess were added as coupling reagents. The reaction mixture was stirred for 24 hours at room temperature. The crude product was collected by filtration. Then, it was purified by dialysis using Dialysis spectra/pro CE float analyzer (MWCO: 100-500 Da).

2.2.3 Deposition of OCT-MUA on AuNPs

OCT-MUA was deposited on the gold surface to form OCT-decorated AuNPs (OCT-AuNPs). In brief, in a 100 ml Erlenmeyer flask, 1 ml (1 mM) stock solution of OCT-MUA was mixed with 20 ml of the prepared AuNPs solution. The pH of the mixture was adjusted to pH 11, incubated under continuous stirring (600 rpm) at room temperature overnight to allow sufficient exchange of citrate anions with OCT-MUA on the particle surface. The formed nanoparticles were purified by centrifugation at $15,700 \times g$ for 20 minutes in a falcon tube using an Avanti centrifuge J-E/ Beckman coulter GmbH, Germany. The supernatant was decanted and the precipitate was resuspended again in Millipore water and recentrifuged. The process was repeated several times.

2.2.3.1 Size and zeta potential measurements by dynamic light scattering

To determine the size, count rate and zeta potential of AuNPs were performed using the Malvern zetasizer nano 6.01 (Malvern Instruments GmbH, Herrenberg, Germany). The sampling time was set automatically. Three measurements were allowed to perform each 10 sub-runs. All measurements were carried out in aqueous solution.

2.2.3.2 UV-VIS spectroscopy

UV-VIS absorbance spectra of the AuNPs-citrate and OCT-AuNPs were recorded using an Uvikon 941 UV-VIS absorbance spectrophotometer (Kontron Instruments GmbH). It was taken five spectra of each gold colloid suspension in the range from 400 to 700 nm. The absorbance measurements were made using 0.5 cm path length quartz cuvettes. The SPR is clearly visible as a peak in the range between 514 and 550 nm.

2.2.4 Cellular uptake of OCT-AuNPs

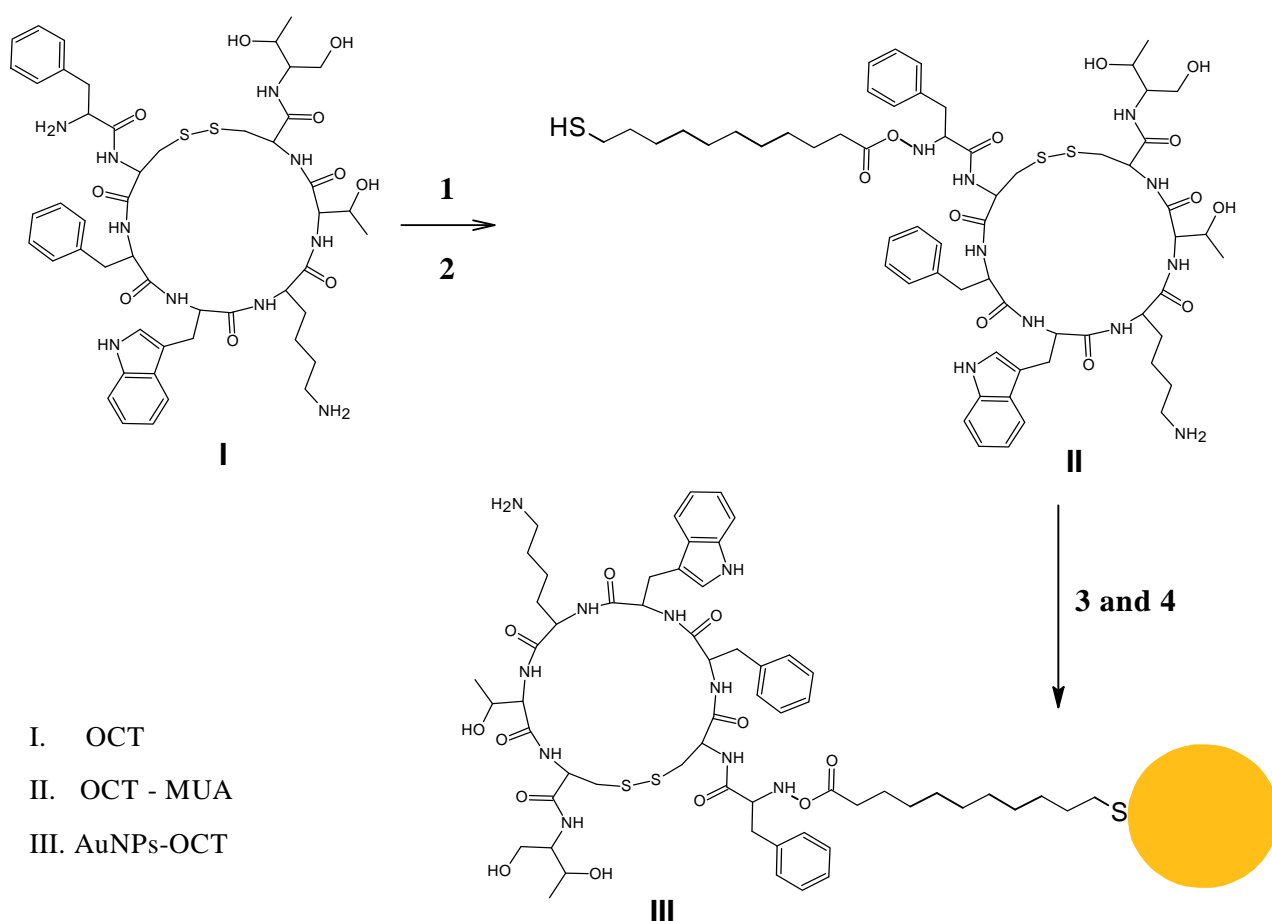
2.2.4.1 Determination of OCT-AuNPs by inductively coupled plasma spectroscopy (ICP-OES)

Pancreatic carcinoid tumor cells (BON-1) which express SSTR2 and SSTR5 was used as a model for quantitative determination of the AuNPs number per cell (29). The selected cells were incubated with 1 ml (50 nM) either unmodified or modified AuNPs for 30 minutes at 37 °C. To investigate the effect of antagonists on the number of internalized NPs, AuNPs-OCT was also incubated in the presence of 100 μl (0.5 mM) antagonist (cyn-164806). The

incubation process was carried out in 1 ml of serum containing culture medium with serum free Leibowitz medium in T-75 tissue culture flasks. To harvest cells, 2 ml trypsin-EDTA was added to the flask. The flasks were incubated at 37 °C for 3 minutes to allow cell detachment. The cells washed with phosphate buffer and centrifuged at 300 ×g (18°C) for 5 minutes, in order to pellet the cells. Then, the harvested cells were transferred to a 5 ml glass vials. The AuNPs concentrations were determined in 96-well plate using an Uvikon 941 UV-VIS absorbance spectrophotometer (Kontron Instruments GmbH) as reported previously (30).

2.2.4.2 ICP-OES sample preparation and determination of AuNPs

This technique is specifically used to determine the concentration of Au³⁺ metals. A mineral acid such as aqua regia was used for dissolution of AuNPs samples. Typically, 500 μl of each sample containing AuNPs was mixed with 200 μl of freshly prepared aqua regia and the volume was completed to 5 ml with Millipore water. The Au³⁺ content of the digested cells was determined using ICP-OES on a JY-70 PLUS (Jobin Yvon Instruments S.A.). The flow rate was 16 ml/minute argon. The concentrations of 1, 10 and 100 ppm gold (III) chloride were used as a standard. To obtain the concentration of AuNPs in solution the number of gold atoms per particles divided measured concentration of Au³⁺ (23, 31).



- I. OCT
- II. OCT - MUA
- III. AuNPs-OCT

Reagents and conditions; 1) 3 ml MUA (1 μM), pH 5-6, BPS; 2) NHS + EDC (2 eq.); 3) AuNPs (20 ml), OCT-MUA (1mM), pH 11, in (H₂O), overnight; 4) Purification (Centrifugation/15,000 g/20 minutes).

Figure 1. Schematic diagram for deposition of OCT onto AuNPs. First MUA was reacted with OCT at its N-terminal. The prepared OCT-MUA was purified by dialysis using Dialysis spectra/pro CE float analyzer (MWCO: 100-500 Da). Then, OCT-MUA was deposited on the gold surface, and then incubated under continuous stirring (600 rpm) at room temperature overnight to allow sufficient exchange of citrate anions with OCT-MUA on the particle surface. The formed nanoparticles were purified by centrifugation at 15,700 ×g for 20 minutes.

3. RESULTS AND DISCUSSION

3.1 Preparation and characterization of AuNPs

3.1.1 Synthesis and characterization of AuNPs

AuNPs (AuNPs-citrate) were synthesized by reduction of HAuCl_4 by trisodium citrate in aqueous medium. Upon addition of trisodium citrate to the HAuCl_4 solution, the color of solution was changed gradually from yellowish color to purple color.

Size (hydrodynamic diameter), Polydispersity index (PDI) and zeta potential of particles are considered as indicative parameters for nanoparticles stability (32-33). PDI is an index represents the size distribution range in colloidal solutions. So, high PDI indicates the heterogeneity of the particle size in the suspension, while smaller PDI values indicate the homogeneity of the particle size in colloids or suspensions. The ideal values of PDI should be less than 0.8. It was reported that PDI below this value indicate that the particle size distribution falls within a narrow range of sizes (32, 34-37). Similarly, both the surface charge and the magnitude of zeta potential play an important role in the stability of the nanoparticles (38).

Regarding the size and zeta potential of the prepared NPs, the results showed that the obtained NPs are uniform and small particle size (20.8 ± 0.5 nm), as illustrated in figure 2. Also, The zeta potential of citrate-AuNPs were measured in Dulbecco's Phosphate-Buffered Saline (DPBS) of pH 7. The results showed that AuNPs-citrate had a high value of a negative surface charge (-68.4 ± 0.5 mV), indicating that the obtained NPs are electrically stabilized with no aggregation (Fig. 6 and 7). This result is in accordance with the previously reported data (39).

In addition, the count rate and PDI were monitored. The recorded high-count rate value (185 kpcs) indicated that the concentration of nanoparticles was high enough for measurements. Also, the values of PDI were very small (0.16), indicating that the colloidal AuNPs were uniform and monodisperse AuNPs, This result is in accordance with the previously reported data (34, 37, 40).

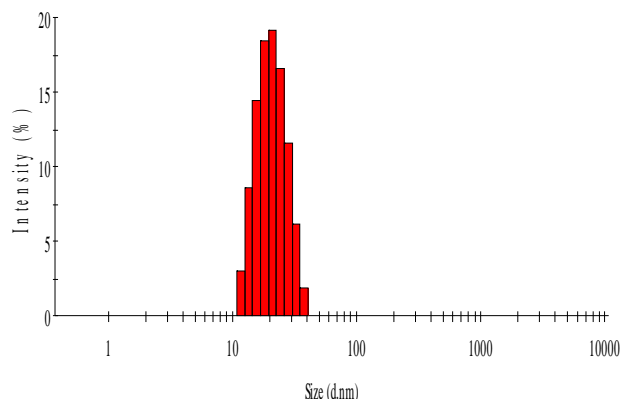


Figure 2 Particle size distribution by intensity of AuNPs measured by dynamic light scattering.

3.1.2 Mono-substitution of Octreotide with 11-Mercaptoundecanoic acid

Since the Lys amine group of OCT is essential for its activity (25, 27), OCT can be substituted at the amine group of its N-terminus instead of the Lys side chain. It has been found that the N-terminus has a pKa of 7.1, while the value of the Lys side chain is 10.1. It was observed that the N-terminus will be reactive in a medium of pH range from 5 to 7, while the amine group in Lys residue was found to be reactive only above pH range 9-10. Therefore, the reaction was established using 11-MUA at low (pH 6) to ensure the substitution or conjugation occurs, selectively, at the N-terminus only, producing mono-substituted OCT-MUA. NHS and EDC were used as coupling reagent. The obtained product was characterized by MALDI-ToF mass spectrometry. The results, illustrated in figure 3, showed that the molecular weight of OCT increased from 1019Da to 1237Da after conjugation of OCT with MUA. These findings match the expected molecular weight of mono-substituted OCT, so it indicates the successful mono-substitution of OCT at acidic pH (Fig. 3).

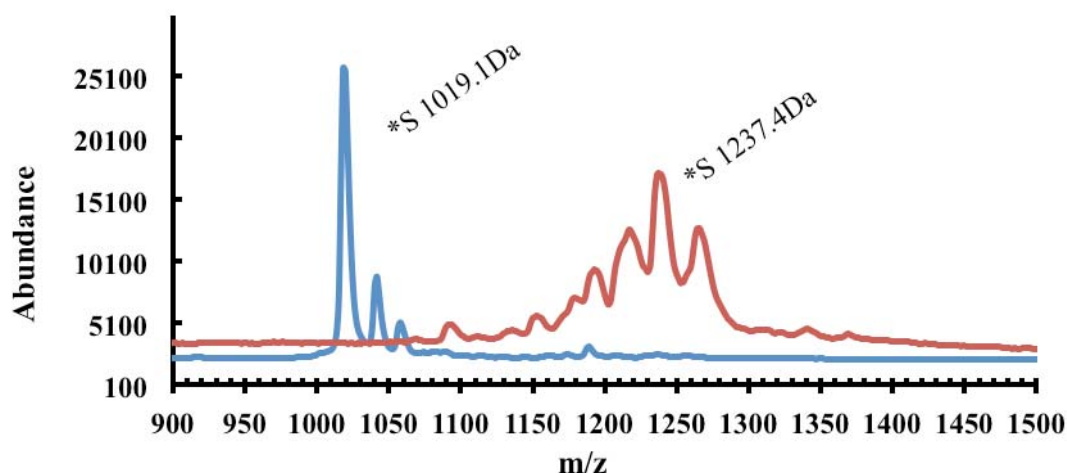


Figure 3. MALDI-ToF mass spectrometry of unmodified and modified OCT with 11-MUA, using IAA/THF as a matrix.

3.1.3 Coating of AuNPs with OCT-MUA

OCT-MUA was deposited on the surface of AuNPs by replacing the citrate with OCT-MUA. In order to obtain well-defined nanoparticles with small hydrodynamic diameter and low PDI, the coating was made in 10 mM NaCl solution (23). Different concentrations of OCT (20, 40, 100, 200, and 300 nM) were used to identify the optimal conditions of OCT coating. The extent of AuNPs coating with OCT could be indicated from the final particle size of the modified NPs. The results, illustrated in figure 4, showed that the particle size (amount of OCT adsorbed) of modified AuNPs increased with the increase of OCT concentration, since the particle sizes increased to $21.7 \pm$

0.06 , 22.4 ± 0.3 , 23.5 ± 0.2 , 25.05 ± 0.07 and 28.3 ± 1.4 for the concentrations of 20 to 300 nM, respectively. Also, it has been observed that the stability of the modified NPs depends on OCT concentration, since the particles are stable up concentration of 200 nM. However, particles, coated with a high concentration of OCT (300 nM), formed aggregates after six hours, indicating the insufficient long-term stability. Therefore, the ideal OCT concentration, used for coating, is 200 nM which keeps the balance between the maximum extent of coating and the maximum stability (no aggregation).

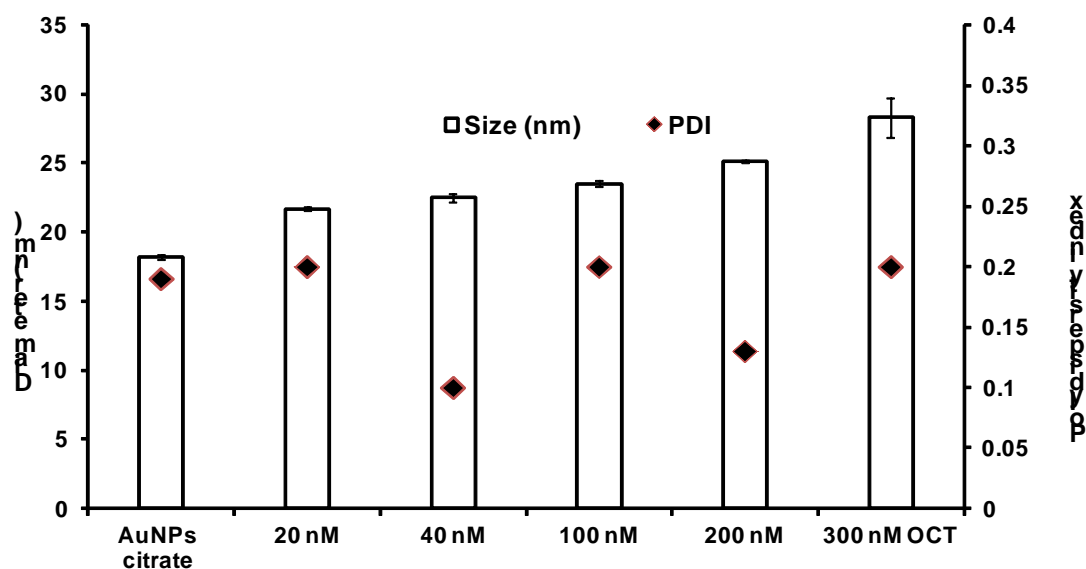


Figure 4 Particle size distribution and polydispersity index of unmodified AuNPs and AuNPs coated with different conc of OCT.

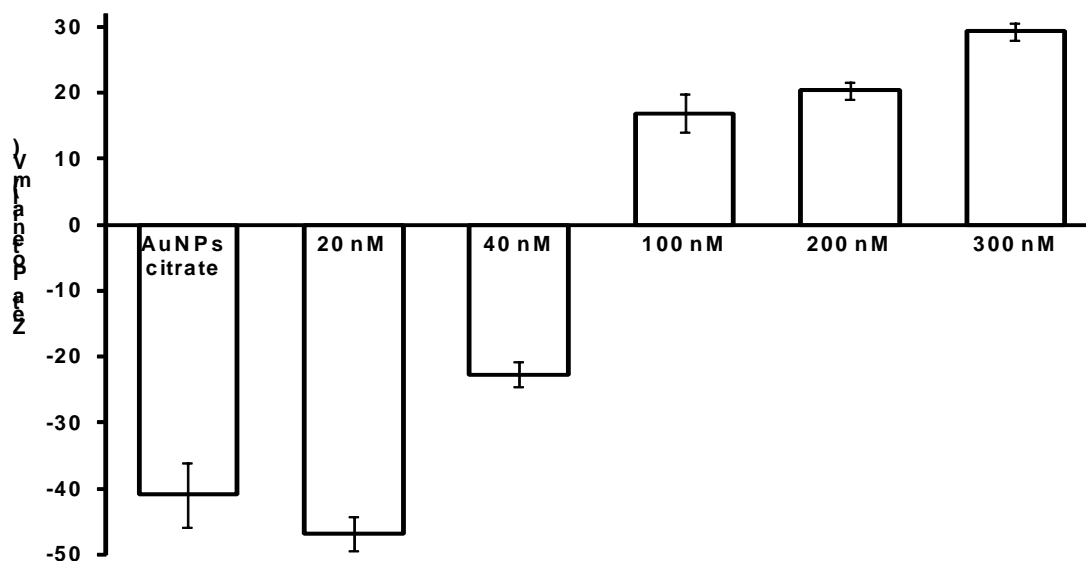


Figure 5. Zeta potential measurements of AuNPs-citrate and AuNPs decorated with OCT. The AuNPs-citrate had a high negative surface charge. After coating with concentrations of (100 to 300 nM) OCT, it became more and more positive.

Zeta potentials were measured to confirm the successful coating of AuNPs with OCT. It was observed that the zeta potential is highly negative (-49 ± 0.8 mV) for AuNPs-OCT. After purification, the zeta potential value increased to become less negative (-41 ± 4.8 mV) as shown in figure 5, but still high enough to stabilize the particles in an aqueous environment. Moreover, the zeta potential of all particle types was initially negative. Then, after coating with concentrations of (100 to 300 nM) OCT, it became more and more positive. AuNPs-OCT at 100, 200 and 300 nM showed the inversion of zeta potential from negative to positive values (16.9, 20.3 and 29.3 mV, respectively (Fig. 5).

Furthermore, the modified AuNPs-OCT was characterized by UV spectroscopy. Figure 6 shows the effect of OCT coating on the surface plasmon resonance peak of AuNPs-citrate. The results showed that the decoration of AuNPs-citrate with OCT was accompanied by a red shift in the surface plasmon resonance peak. Similar finding was obtained and reported by other group since the red shift was attributed to the deposition of OCT and a size increase of nanoparticles (41). The SPR is clearly visible as a peak at 517 and 522 nm for AuNPs-citrate and AuNPs-OCT respectively.

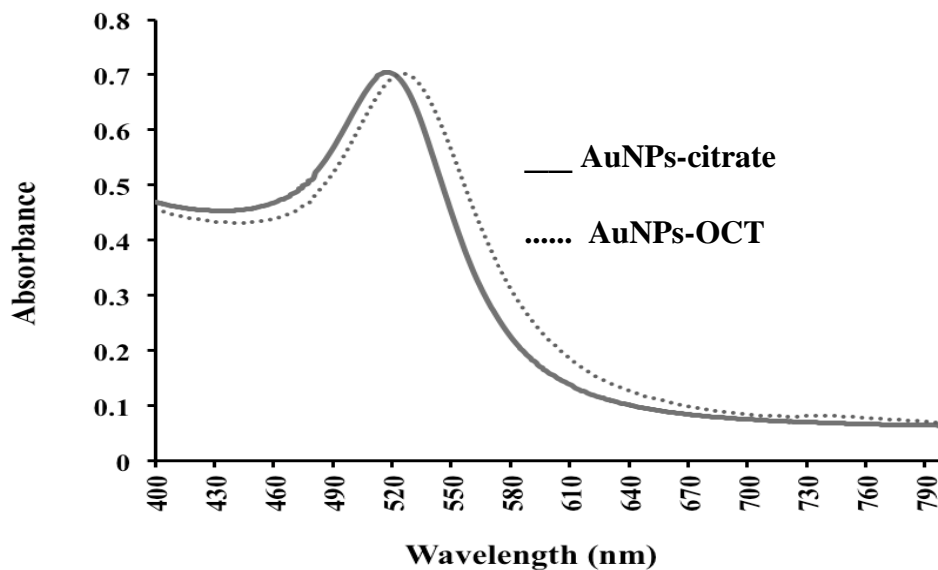


Figure 6. UV-VIS spectra of AuNPs-citrate and purified AuNPs decorated with OCT. The SPR is clearly visible as a peak at 517 and 522 nm for AuNPs-citrate and AuNPs-OCT respectively.

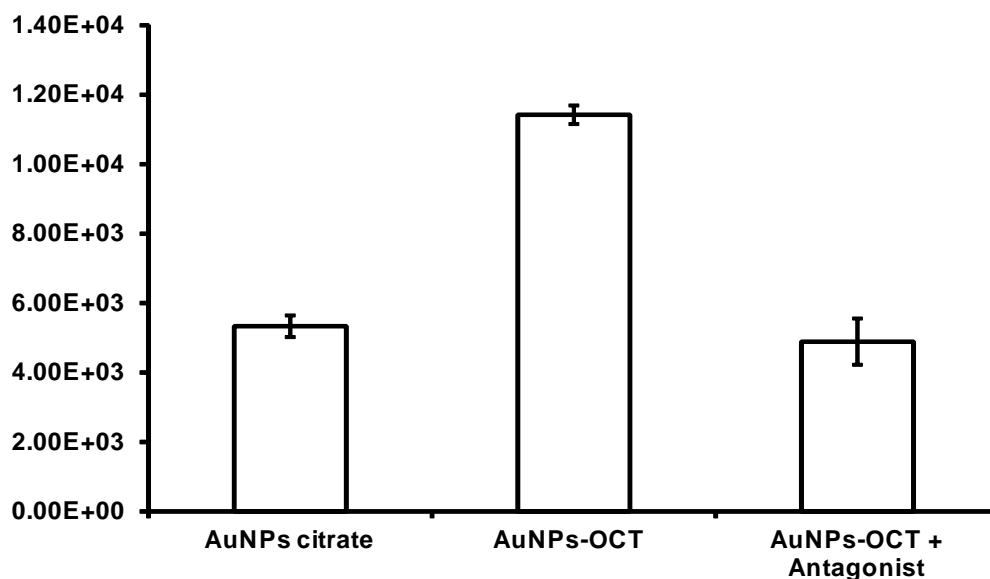


Figure 7 The cellular uptake of AuNPs. Both modified and unmodified AuNPs. The results were calculated from the average of three experiments.

3.1.4 Cellular uptake of OCT-AuNPs

Since all kinds of the formulated AuNPs are of nearly similar sizes but possess different outer layers, this suggests that surface properties may strongly affect the interactions with the cells. The initial concentration of AuNPs in the culture medium was 162 pmol for either AuNPs-citrate or AuNPs-OCT. The selected modified NPs was that contains OCT of 200 nM (particle size equal 25.1 nm). The results showed that AuNPs-OCT were internalized in higher amounts (estimated number, $11400 \pm 303/\text{cell}$) compared to AuNPs-citrate (estimated number 5330 ± 265). Interestingly, it has been observed that the addition of an antagonist (cyn 154806) led to huge reduction of the number of the internalized particles, since the estimated number was nearly similar to the unmodified NPs. (estimated number 5330 ± 265 (Fig. 7).

Although, the modified NPs showed the higher particle size (25 nm) than the unmodified one (18 nm) it showed a higher extent of internalization. also, the selected antagonist at certain concentration (1 mM) displaced the nanoparticles from the receptor. So, the difference in the cellular uptake of AuNPs-OCT could be attributed to the differences in surface properties and not due to the difference in size.

4. CONCLUSIONS

this work has successfully demonstrated that SSTRs not only assist in drug therapy but also have a great role in targeted delivery of nanoparticles to specific cells. In this study, the results indicated that nanoparticles loaded OCT as a selectively agonist targeted and delivered to the specific sites with high efficacy. OCT can deliver the nanoparticles to the targeted sites with high drug delivery efficacy in vitro. All analytical results indicated a successful coating of AuNPs with OCT with an average size of AuNPs and AuNP-OCT. Additionally, an inversion of the zeta potential to a positive charge indicates the deposition of OCT. The UV absorbance spectra showed a red shift in the surface plasmon resonance peak of AuNPs-OCT compared with the AuNPs. Furthermore, ICP-OES showed that the number of AuNPs-OCT per cell is significantly higher compared to AuNPs-citrate or AuNPs-OCT in the presence of antagonist. Antagonist can suppress the binding of the OCT-decorated AuNPs, indicating that the binding of OCT-decorated nanoparticles to cells is due to receptor-specific binding.

The obtained results in this report allow us to understand how nanoparticles target specific sites in the body with specific targeting peptides. Consequently, this gives a better understanding of the delivery to the targeted sites with reduced side effects and high drug delivery efficacy.

ACKNOWLEDGEMENTS

I would like to thank Dr. Abdellatif bouazzaoui for supplying us with cell lines expressing SSTRs and Fouad Darras for his assistance in the chemistry part and proofreading,

BIBLIOGRAPHY

1. P. P. Surujpaul *et al.*, *Biophys Chem* **138**, 83 (Dec, 2008).
2. B. Duncan, C. Kim, V. M. Rotello, *J Control Release* **148**, 122 (Nov 20, 2010).
3. N. Khlebtsov, L. Dykman, *Chem Soc Rev* **40**, 1647 (Mar, 2011).
4. H. L. Watt, G. Kharmate, U. Kumar, *Mol Cell Endocrinol* **286**, 251 (May 14, 2008).
5. P. Dasgupta, *Pharmacol Ther* **102**, 61 (Apr, 2004).
6. Y. A. Zhang, X. Q. Wang, J. C. Wang, X. A. Zhang, Q. A. Zhang, *Pharmaceutical Research* **28**, 1167 (May, 2011).
7. Y. Zhang *et al.*, *Biomaterials* **33**, 679 (Jan, 2012).
8. V. Rufini, M. L. Calcagni, R. P. Baum, *Semin Nucl Med* **36**, 228 (Jul, 2006).
9. Y. Taniyama *et al.*, *Endocr J* **52**, 605 (Oct, 2005).
10. Y. C. Patel, *Front Neuroendocrin* **20**, 157 (Jul, 1999).
11. J. B. Long, *Eur J Pharmacol* **149**, 287 (May 10, 1988).
12. A. Aiboushev *et al.*, *Photochem Photobiol Sci*, (Oct 10, 2012).
13. X. Hong, E. A. Hall, *Analyst* **137**, 4712 (Oct 21, 2012).
14. E. E. Bedford, J. Spadavecchia, C. M. Pradier, F. X. Gu, *Macromol Biosci* **12**, 724 (Jun, 2012).
15. M. Hojeij, N. Younan, L. Ribeaucourt, H. H. Girault, *Nanoscale* **2**, 1665 (Sep, 2010).
16. L. Dykman, N. Khlebtsov, *Chemical Society Reviews* **41**, 2256 (2012).
17. M. De Simone *et al.*, *Journal of Peptide Science* **16**, 200 (Sep, 2010).
18. B. Kang, M. A. Mackey, M. A. El-Sayed, *J Am Chem Soc* **132**, 1517 (Feb 10, 2010).
19. R. Prades *et al.*, *Biomaterials* **33**, 7194 (Oct, 2012).
20. S. Bhattacharyya *et al.*, *Advanced Materials* **23**, 5034 (Nov 16, 2011).
21. J. Kimling *et al.*, *J Phys Chem B* **110**, 15700 (Aug 17, 2006).
22. G. Frens, *Nature-Phys Sci* **241**, 20 (1973).
23. A. Elbakry *et al.*, *Nano Lett* **9**, 2059 (May, 2009).
24. D. H. Na, S. B. Murty, K. C. Lee, B. C. Thanoo, P. P. DeLuca, *AAPS PharmSciTech* **4**, E72 (Dec 31, 2003).
25. D. H. Na, P. P. DeLuca, *Pharm Res* **22**, 736 (May, 2005).
26. E. J. Park, D. H. Na, *Anal Biochem* **380**, 140 (Sep 1, 2008).
27. D. H. Na, K. C. Lee, P. P. DeLuca, *Pharm Res* **22**, 743 (May, 2005).
28. Y. J. Pu *et al.*, *Organic Process Research & Development* **13**, 310 (Mar-Apr, 2009).
29. E. Ludvigsen *et al.*, *Med Oncol* **21**, 285 (2004).
30. W. Haiss, N. T. Thanh, J. Aveyard, D. G. Fernig, *Anal Chem* **79**, 4215 (Jun 1, 2007).
31. B. D. Chithrani, A. A. Ghazani, W. C. W. Chan, *Nano Lett* **6**, 662 (Apr, 2006).
32. J. Pereira-Lachataignerais *et al.*, *Chem Phys Lipids* **140**, 88 (Apr, 2006).
33. C. M. Moraes, E. De Paula, A. H. Rosa, L. F. Fraceto, *Journal of the Brazilian Chemical Society* **21**, 995 (2010).
34. M. Aghajani, A. R. Shahverdi, A. Amani, *AAPS PharmSciTech*, (Sep 21, 2012).
35. G. Lewis, Y. Li, *J Mech Behav Biomed Mater* **3**, 94 (Jan, 2010).
36. C. Rosenfeld, C. Serra, C. Brochon, G. Hadziioannou, *Lab Chip* **8**, 1682 (Oct, 2008).
37. J. Vieville, M. Tanty, M. A. Delsuc, *J Magn Reson* **212**, 169 (Sep, 2011).
38. E. D. Kaufman *et al.*, *Langmuir* **23**, 6053 (May 22, 2007).
39. R. Greenwood, K. Kendall, *Journal of the European Ceramic Society* **19**, 479 (1999).
40. X. Liu, H. Xu, H. Xia, D. Wang, *Langmuir* **28**, 13720 (Sep 25, 2012).
41. A. Elbakry *et al.*, *Nano Lett* **9**, 2059 (May, 2009).